Chemical Engineering Science 247 (2022) 117006

Contents lists available at ScienceDirect

Chemical Engineering Science

journal homepage: www.elsevier.com/locate/ces

Improvement in mixing efficiency of microfluidic passive mixers functionalized by microstructures created with proton beam lithography

Emad Nady, Gyula Nagy, Róbert Huszánk *

Institute for Nuclear Research (Atomki), P.O. Box 51, H-4001 Debrecen, Hungary

HIGHLIGHTS

- Different microfluidic devices were designed, simulated and made for micro-mixing purposes.
- Microstructures were integrated into PDMS microfluidic devices from the same material.
- The fine 3D microstructure were created by focused ion beam lithography.
- The mixing efficiencies were improved, in some cases to near 100%, keeping the size of the chip in a few mm.
- The presented method opens the opportunity to further improve mixing efficiencies and to further decrease chip dimensions.

ARTICLE INFO

Article history:
Received 17 May 2021
Received in revised form 25 July 2021
Accepted 8 August 2021
Available online 11 August 2021

Keywords:
Proton beam writing
Microfluidics
Microfluidic passive mixers

ABSTRACT

In this work, different microfluidic passive mixer devices were designed, simulated and realized. The mixing unit area was functionalized by microstructures, whose shapes and layouts were designed in the simulations to improve the mixing efficiency of the chips. It is known that a micro wall array is a promising tool for mixing in a microfluidic passive mixer device. In the present work, the length and the areal density of the walls in the micro wall array were varied in order to find good mixing performance. The devices were then created with ion microlithography and UV lithography techniques. Mixing test were performed from which the mixing efficiencies were determined. It was found, that the mixing efficiency of the fabricated passive micromixers can be improved to an excellent value by more densely distributed and longer micro-walls.

1. Introduction

Microfluidic devices have become important part of technology nowadays in numerous fields of application, such as chemical reactions, biosensors, synthesis of nanomaterials, diagnostic device for detection of biological samples, etc. These devices are characterized by small dimensions and high surface to volume ratio, so that they offer unique and very different physical characteristics comparing to the macroscopic world. In microfluidic devices, micromixers are used to mix two or more fluids. Mixing of two different fluids in microchannels is difficult, because of the laminar flow (i.e.: Reynolds number, *Re* is typically smaller than 100). In this case, mixing between parallel fluid flows (i.e.: perpendicular to the flow direction) occurs only by molecular diffusion, because convective mass transfer takes place only in the direction of the fluid flow. (Beebe et al., 2002).

In general, micromixers can be classified into two types: active and passive. (Hessel et al., 2003; Sullivan et al., 2007; Knight et al., 1998; Bessoth et al., 1999; Stroock et al., 2002; Wang et al., 2007; Hassell and Zimmerman, 2006; Fu et al., 2006; Sato et al., 2005). In the mixing process, active micromixers need external turbulence effects such as electrokinetics, dielectrophoretics, electrohydrodynamics, temperature, pressure, etc. (Yang et al., 2001; Bau et al., 2001; Lin et al., 2005; Tsouris et al., 2003; Fu et al., 2005) Hence, the structures of active micromixers are often complicated. On the other hand, the passive-type mixers are mainly based on breakup, folding, fluid stretch, and molecular diffusion. This results a simpler fabrication process, but, in spite of this, their mixing efficiency can approach that of the active mixers. (Hong et al., 2004; Liu et al., 2004; Goullet et al., 2006; Park et al., 2004; Jiang et al., 2004; WONG et al., 2004; Chen and Meiners, 2004)

* Corresponding author.
E-mail address: huszank@atomki.hu (R. Huszánk).

https://doi.org/10.1016/j.ces.2021.117006
0009-2509/

1.1. Passive micromixers

Most passive micromixers have various micro-structures with which high mixing performance can be achieved with low pressure drop and a short mixing length. Passive micromixers rely on molecular diffusion and chaotic advection phenomena of mass transport. The best way to maximize the mixing efficiency of a micromixer is to decrease the diffusion path. By varying the design, it will allow to manipulate the laminar flow within the channels, so the enhancement of chaotic advection can be realized. A shorter diffusion path will increase the mixing efficiency.

There are many studies about passive micromixers utilizing simple planar structures such as obstacles, unbalanced collisions, convergence–divergence, and spiral channel layouts, among others, and their results shows acceptable range for mixing efficiency (79–95%). Several experimental and theoretical investigations have been carried out for different passive micromixers in the last decades.

Different types of mixing mechanism can be found in the literature about passive micromixers, as following:

a. flow lamination, which is used in basic T-mixer and Y-mixer Bothe et al., 2011; Kamholz, 1999; Swickrath et al., 2009; Chen et al., 2011 using different geometries: zig-zag, square-wave, rhombic and similar (Hossain et al., 2009), in serial multi-stage and multi-layer mixers (Tofteberg et al., 2010);
b. chaotic mixing by eddy formation, stretching and folding (Kim and Ansari, 2007; Kim et al., 2010; Shih and Chung, 2008; Xu et al., 2011; Cho et al., 2011; Yu et al., 2011; Afzal and Kim, 2014);
c. split-and-recombine concepts (SAR) (Ohkawa, 2008; Lee and Lee, 2008; Chen et al., 2009; Chen et al., 2011; Nimafar et al., 2012), etc.

Mixing performance enhancement can be achieved in passive micromixers by optimizing the structural dimensions of the microchannel in such a way that the mixing performance is improved. There are various structural dimensions were reported in a review article (Cai et al., 2017), that can be used to improve the mixing efficiency. The design of a Y-shaped micromixer, with rectangular and triangular barriers, was designed and introduced to mix fluids with small diffusion coefficient molecules, and the resulted mixing efficiency is *100 %* at a flow rate corresponding to the Reynolds number (*Re*) of *25*. (Karthikeyan et al., 2017) An experimental study was performed employing split and recombination micromixer, *T*-type and *O*-type mixers, with Reynolds number ranging from 0.083 to *4.166* and the corresponding mixing efficiency can be reached to *90 %* in a short length. (Nimafar et al., 2012)

A numerical evaluation of a passive micromixer with Reynolds numbers ranging from *0.1* to *60,* using cylindrical restrictions within a curved microchannel, found that the mixing efficiency values were *72% – 88%* (Alam et al., 2014). With a three-dimensional, staggered herringbone shaped micromixer, optimized for mixing of two fluids, with low diffusion coefficient, less than *90 %* of mixing efficiency was obtained (Afzal and Kim, 2014) T type three-dimensional designs of twisted microchannels were constructed and numerically simulated as a chaotic mixers. (Jen et al., 2003) Numerical calculations and practical tasks on a planar serpentine micromixer have been evaluated using chaotic mixing, and yielded *90%* of mixing efficiency at *Re* of *2*. (Tung et al., 2009)

A passive micromixer with deformable baffles was examined numerically and the achieved mixing efficiency was *98%* at the *Re* from *0.01* to *300*. (Madhumitha et al., 2017) Micromixer was fabricated using *PDMS* as material by a lithography process, in which, the staggered herringbone chaotic layout was designed and experimented, and the mixing efficiency of *99.7 %* at 20 μl/min and *99.2% at* 100 μl/min was resulted. (Chen and Wang, 2015) Numerical simulation and experimental study of split and recombine micromixer have also been studied and *84%* of mixing efficiency was achieved. (Wang et al., 2016).

Numerical simulation and experimental study of tesla valve micromixer was investigated and mixing efficiency of *95.3% was* achieved at *Re* of *1*. (Wang et al., 2014) A three-dimensional chessboard shape micromixer was reported with a *95%* of mixing efficiency at 12.7 μl/min. (Cha et al., 2006) A micromixer device for lab on chip application was developed by *UV* cured adhesive bonding technique. (Kapilmanoharan and Lekurwale, 2014) *SU-8* used to fabricate a micromixer device where a bonding process was developed using *SU-8* coated over the substrate. (Svasek et al., 2004) A three-dimensional spring like micromixer device was experimented and it was bonded to the substrate using a controllable furnace (Saragih and Ko, 2009).

In this work passive micromixers, consisting of a circular frame filled with obstructions, were studied, and their mixing performance were investigated by Finite Element Method (Comsol Multiphysics). The different obstructions were simulated, optimized and designed for real chip micromixers. The functionalization of the mixers with the optimized obstructions were realized by proton beam lithography. The mixing efficiencies in the real chips were measured and calculated by spectrophotometric method.

2. Methodology

2.1. COMSOL simulation

Computational Fluid Dynamics (CFD) simulations were conducted using Comsol Multiphysics version 5.3a, with which the designs of our passive micromixers presented in our earlier work (Nady et al., 2021) were further improved. During the simulation, water and a diluted aqueous solution are injected to the mixer through two inlets. They flow through the chip, including the mixing unit area, where they start to mix together. The level of the mixing depends on the mixer designs and parameters.

The simulated geometries and dimensions of two-dimensional proposed designs are shown in Fig. 1. The main parts of the micromixers are *2* inlets, *2* outlets, a mixing unit area and straight channels that connects the inlets and the outlets with the mixing unit area with length (L) = 2 mm.

As shown in Fig. 1, the proposed mixing unit areas are:

- *SC*: simple circle, radius (*r*) = 1 mm,
- *CLSW:* circle with low number and same level walls, wall thickness (*T*) = 0.03 mm, gap between walls (*G*) = 0.17 mm,
- *CHSW:* circle with high number and same level walls, wall thickness (*T*) = 0.03 mm, gap between walls (*G*) = 0.07 mm,
- *CLTW:* circle with low number and tall walls, wall thickness (*T*) = 0.03 mm, gap between walls (*G*) = 0.17 mm and
- *CHTW:* circle with high number and tall walls, wall thickness (*T*) = 0.03 mm, gap between walls (*G*) = 0.07 mm.

The *creeping flow* and *transport of diluted species* modules were applied to perform the mixing simulations for the two-dimensional designs. The governing equations used in these modules are presented in *equations 1–3*. The flow of an incompressible Newtonian liquid in micromixer can be described by the Navier-Stokes and continuity equations, shown in *equations (1) and (2)*, respectively,

$$\nabla\left[-pI+\mu(\nabla u+(\nabla u)^{T})\right]+F=0 \tag{1}$$

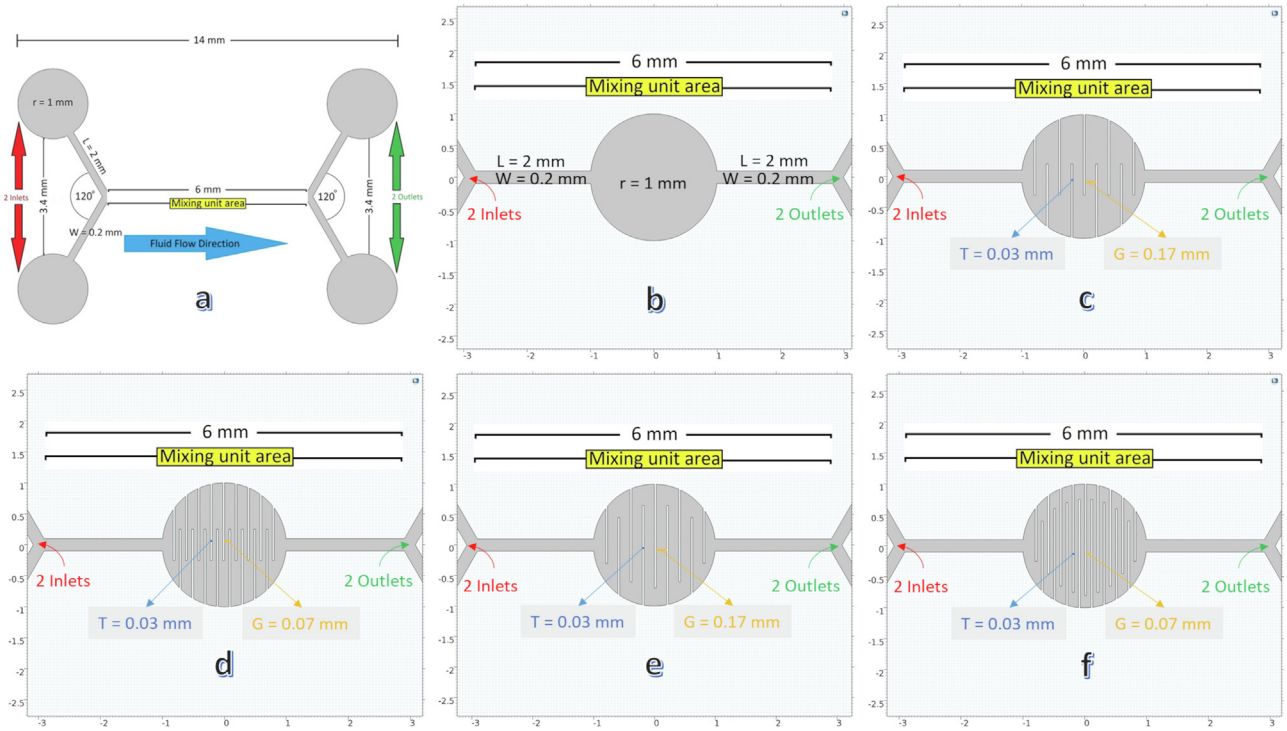

Fig. 1. Geometry of the main parts of the micromixers : a) inlets, outlets and mixing unit area, b) simple circle [SC], c) circle with low number and same level walls [CLSW], d) circle with high number and same level walls [CHSW], e) circle with low number and tall walls [CLTW], and f) circle with high number and tall walls [CHTW]. T is the wall thickness (30 um in all cases), G is the gap between the walls.

$$\rho\nabla(u) = 0 \tag{2}$$

where p is the fluid pressure, μ is the dynamic viscosity of the fluid, I is the identity matrix, T is viscous stress tensor, F is the body force, ρ is the fluid density and u is the flow velocity.

The transport of the solved molecules in the systems can be described by the convection – diffusion equation as shown in *equation (3)*,

$$\nabla(-D\nabla c) + u\nabla c = R \tag{3}$$

where D and c are the diffusion constant and the concentration of the species, respectively, and R is the source term.

2.2. Microfluidic chip fabrication

The proposed microfluidic mixer chips were realized using the combination of UV soft lithography and proton beam microlithography (PBW). This process can be found in detail in our earlier work (Nady et al., 2021), here we give only a brief description. The microstructures for the mixing unit area were created in a poly (dimethyl-siloxane) (PDMS) base layer by proton beam lithography. The microfluidic channels, inlets and outlets and the cap for the mixing unit area were fabricated by UV lithography, also from PDMS polymer. It has been taken into account that the heights of the fabricated microstructure (mentioned in Table 1) should be fitting to the depth of the caps, so the base and the cap parts (have the same height and depth) are bonded together chemically by plasma treatment. By this way, the height of the channels (or any part of the chip) after bonding is equal to the mentioned height of the microstructure in the table.

Fig. 2 shows the electron microscopic images of the four different mixing unit areas created by PBW technique, while Fig. 3 shows the optical microscopic images of the fully assembled chips. These chips were used to measure the mixing efficiencies as follows: water was injected into one inlet and diluted methylene blue aqueous solution into the other. The methylene blue solution concentration is low enough (2×10^{-5} mol/dm^3) that its parameters can be considered equal to that of water.

The mixed samples at the outlets were collected for all the different micromixers, then the concentrations of the collected samples were measured using UV/vis spectrophotometry. There is a linear relationship between the absorbance (A) and the concentration. This was firstly described by the Lambert-Beer law, *equation 4*, where c is the concentration, ε is the molar absorption coefficient and l the optical path length in cm.

$$A = \varepsilon c l \tag{4}$$

Table 1
Results of mixing efficiencies for different mixer designs.

Structure	Mixing unit area dimensions (Width / Height)(*μm / μm*)	Inlets and outlets dimensions (Width / Height)(*μm / μm*)	Flow Rate Range (*μL/min*)	Reynolds Number Range	Concentration outlet 1 (mol/dm^3) at flow rate = 1 μl/min	Concentration outlet 2 (mol/dm^3) at flow rate = 1 μl/min	Mixing Efficiency (%) at flow rate = 1 μl/min
SC[53]	*2000/65*	*200/65*	*1–6*	*0.19–1.15*	0.291×10^{-5}	1.709×10^{-5}	*29.11*
CLSW	*170/28*	*200/28*	*1–6*	*0.43–2.61*	0.637×10^{-5}	1.363×10^{-5}	*63.67*
CHSW	*70/27*	*200/27*	*1–6*	*0.49–2.96*	0.959×10^{-5}	1.041×10^{-5}	*95.86*
CLTW	*170/25.5*	*200/25.5*	*1–6*	*0.51–3.06*	0.817×10^{-5}	1.183×10^{-5}	*81.72*
CHTW	*70/27*	*200/27*	*1–6*	*0.49–2.96*	0.971×10^{-5}	1.029×10^{-5}	*97.08*

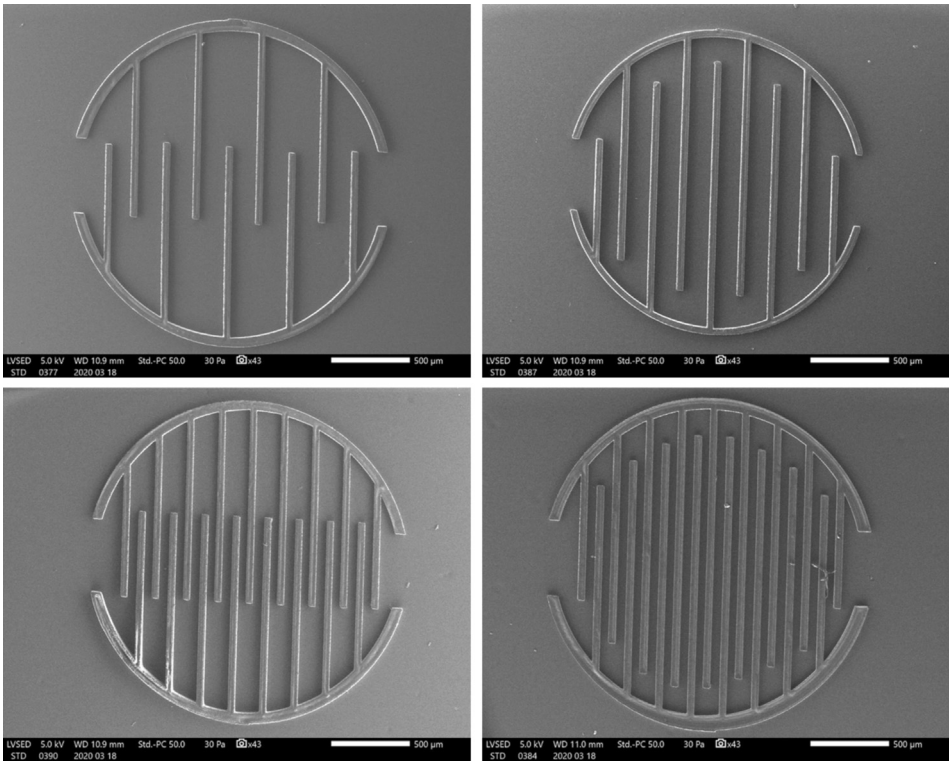

Fig. 2. The electron microscopic image of the real different mixing unit areas (CLSW, CHSW, CLTW and CHTW), created by PBW technique.

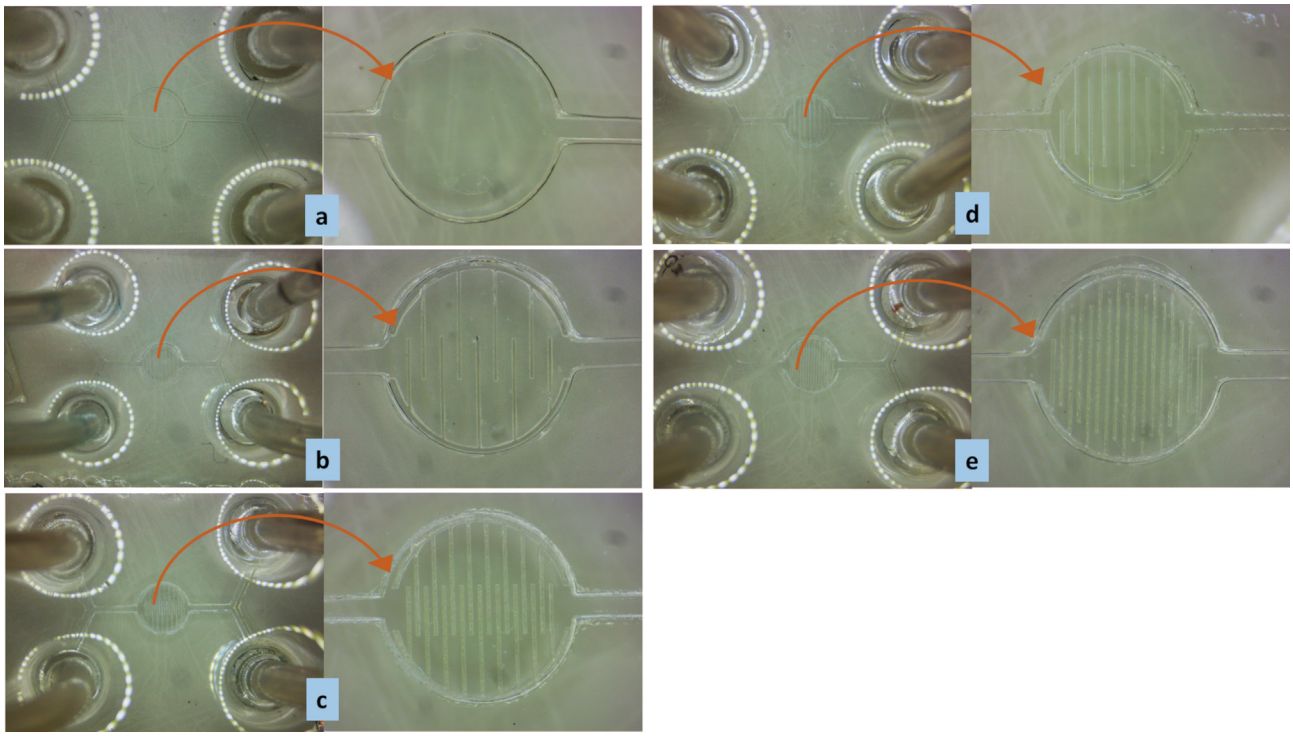

Fig. 3. Top view of the whole microfluidic chips (pipes + PDMS cap bonded to PDMS microstructures) for different mixing microstructures, and high magnification photos of the mixing unit area of PDMS microstructures: a. SC, b. CLSW c. CHSW d. CLTW and e. CHTW.

After the mixing of the two fluids, the mixed fluids were collected for absorbance measurements. Consequently, the concentrations of the two fluids can be determined using the *equation 4*. The mixing efficiency (*M*) of the micromixers can be calculated using *equation (5)*. (Cai et al., 2017).

In the case of COMSOL simulations all data point were exported point by point, not only the endpoints. Then, we use the *equation* (5) to calculate the mixing efficiency at every point, and then make an average from them. Though, in the case of the experimental measurements, we collect the outlets separately in two sample holders and we have only two values after measuring the absorbance. From the two point, knowing the concentrations, the mixing efficiency can be calculated directly:

$$M = \left[1 - \sqrt{\left(\frac{c_{out} - \bar{c}_{out}}{\bar{c}_{out}}\right)^2}\right] \times 100\% \quad (5)$$

where c_{out} is one of the outlet concentrations and $\bar{c}_{\mathrm{out}}$ is the average concentration of the two outlet concentrations (Cai et al., 2017). The average concentration is the half concentration of the initial c_0 concentration, which is 1×10^{-5} mol/dm^3. The mixing efficiency is always compared to this by one of the outlet concentration, as in *equation (5)*. The average of the outlets will be also always the half concentration of the inlet.

In accordance with *equation (5)*, the mixing efficiency *M = 0 %* indicates completely unmixed state of the solved molecules, i.e. concentrations at the two outlets correspond to the concentrations at the two inlets, while *M = 100 %* indicates the completely mixed state, i.e. the concentrations at the two outlets are equal to each other. For practical applications, the acceptable range for efficiency of mixing is between *80 and 100%*.

3. Results and discussion

3.1. COMSOL simulation and mixing efficiency

The fluid flow and mixing properties of different 2-dimensional designs (illustrated in Fig. 1) were simulated.. The value of molecular diffusion coefficient using in this model is fixed at 10^{-11} m^2/s. The molar concentration of the two fluids entering the two inlets are set to *0* and *100* mol/m^3. The fluid velocities at the inlets were set to 0.01 m/s. The simulations of the mixing in the proposed mixer designs are presented in Fig. 4. The left hand panel of each figure shows the concentration distribution, while the right hand panels show concentration profiles at the indicated cross-sections (cut lines).

The indicated two cut lines (distance = 0) and (distance = 5), shown in Fig. 4, were used to find the mixing efficiency values around the inlets and outlets of micromixers respectively.

The value of concentration at each point of the cut line of each micromixer separately was exported from the simulated data. Then by *equation (5)*, the initial concentration (c_0) = *100* mol/m^3 and the average concentration = *50* mol/m^3, the mixing efficiency for each point of the cut line was calculated individually, and averaged.

The results showed that the efficiency of mixing was poor and its value was *38.17 %* for simple circle [*SC*], while it improves for higher values *73.18 %* for circle with low number and same level walls [*CLSW*] but still below the accepted range of mixing efficiency. The accepted value *91.36 %* of mixing efficiency can be obtained by low number and tall walls [CLTW], while excellent values of mixing efficiency *99.45 %* and *99.99 %* were achieved using micromixer circle with high number and same level walls [*CHSW*] and circle with high number and tall walls [*CHTW*] respectively.

As a conclusion, the simulations predict inefficient mixing in the case of the [SC] and [CLSW] mixer designs, while it improves in the case of [*CLTW*] and reaches the maximum mixing in case of [*CHSW*] and [*CHTW*] chips.

3.2. Microfluidic chip test

A syringe-pump was used to pump the two fluids at the inlets with different flow rate (from *1* to 6 μl/min*)*. The fluids (water and diluted aqueous solution of methylene blue) density and viscosity are *1000 kg/m^3* and *10^{-3} kg/ (m.s)*, respectively. The concentration of the methylene blue solution is low enough (initial concentration (c_0) = 2×10^{-5} mol/dm^3) that its parameters can be considered equal to that of water. The mixed samples were collected at the outlets. The concentration of these samples were measured by UV/vis spectrophotometry. Then, the mixing efficiency (M) was calculated using *equation (5)*.

All of the fabricated microfluidic chips, the simple circle [SC], circle with low number and same level walls [CLSW], circle with high number and same level walls [CHSW], circle with low number and tall walls [CLTW] and circle with high number and tall walls [CHTW] micromixers are shown in Fig. 5.

The result of the mixing efficiency calculations for all the mixer designs are summarized in Table 1.

The velocity (V) of the fluids through the designed micromixer, described by the following *equation (6)*, depends on the flow rate (Q) and the hydraulic diameter of the used structure (D_h). The D_h can be calculated using *equation (7)*, where (a) and (b) are the height and the width of the designed walls, respectively. The calculated results of velocity were listed in Table 1,

$$V = \frac{4Q}{\pi D_h} \quad (6)$$

$$D_h = \frac{2ab}{a+b} \quad (7)$$

The Reynolds number were calculated for all design and geometries as a function of the flow rates (1–6 μl/min). The calculations showed that R_e ranges 0.19–1.15, 0.43–2.61, 0.49–2.96, 0.51–3.06 and 0.49–2.96 for SC, CLSW, CHSW, CLTW and CHTW, respectively. This low value of *Re* indicates that in our work the flow is laminar.

Mixing efficiencies were calculated for a range of flow rates in case of all mixer designs. Fig. 6 show the results.

As illustrated in Fig. 6, the graphs show that the mixing efficiency is decreasing when the flow rate increases for all micromixers.

From Fig. 6, the values of mixing efficiency at flow rate 1 μl/min were *29.11 %, 63.67 %, 95.86 %, 81.72 % and 97.08 %* for the micromixers SC, CLSW, CHSW, CLTW and CHTW respectively. The highest mixing efficiency can be achieved using CHSW and CHTW micromixers due to the fact of its geometry, which increases the surface area between the different fluids and decreases the diffusion path. This is a considerable improvement in the mixing efficiencies comparing to the microfluidic passive mixers functionalized by microstructures of our earlier work (Nady et al., 2021).

The trend of the measured mixing efficiencies of the geometries agreed well with the trend of the simulated mixing efficiencies, i.e.: increasing order of the mixing efficiency as a function of the geometry is SC, CLSW, CLTW , CHSW and CHTW for both the simulation and the experiment.

4. Conclusions

In this work, different microfluidic passive mixer devices were designed, simulated and realized. The mixing unit area was functionalized by microstructures, whose shapes and layouts were

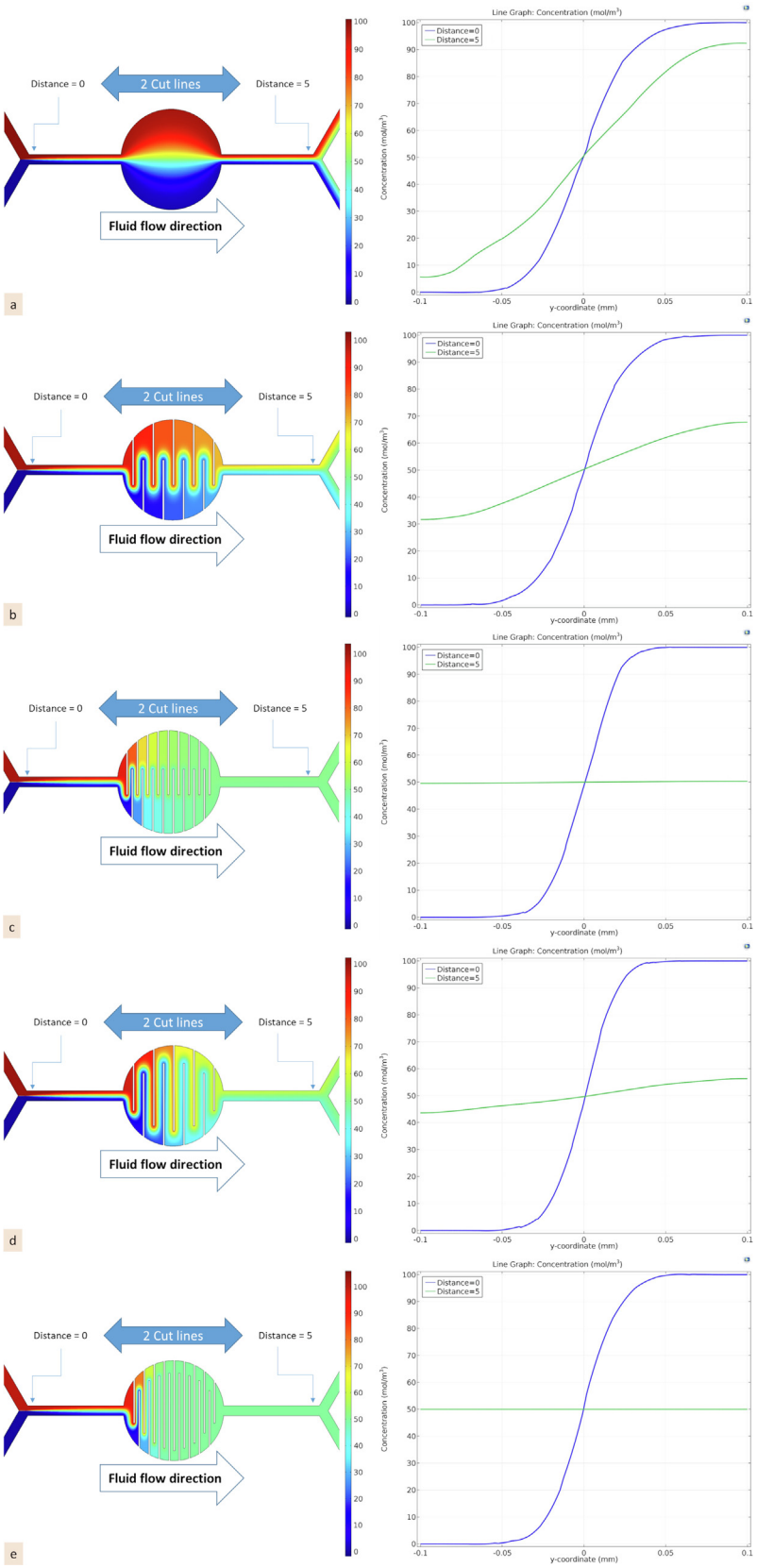

Fig. 4. Left: COMSOL simulation of mixing of two fluids for **a**. Simple Circle structure (SC), **b.** Circle with Low number and same level Walls structure (CLSW), **c.** Circle with High number and same level Walls structure (CHSW), **d.** Circle with Low number and Tall Walls level Walls structure (CLTW), and **e.** Circle with High number and Tall Walls structure (CHTW). Right: Concentration profile for distance = 0 (blue line) and distance = 5 (green line) for a. (SC), b. (CLSW), c. (CHSW), d. (CLTW), and e. (CHTW), respectively.

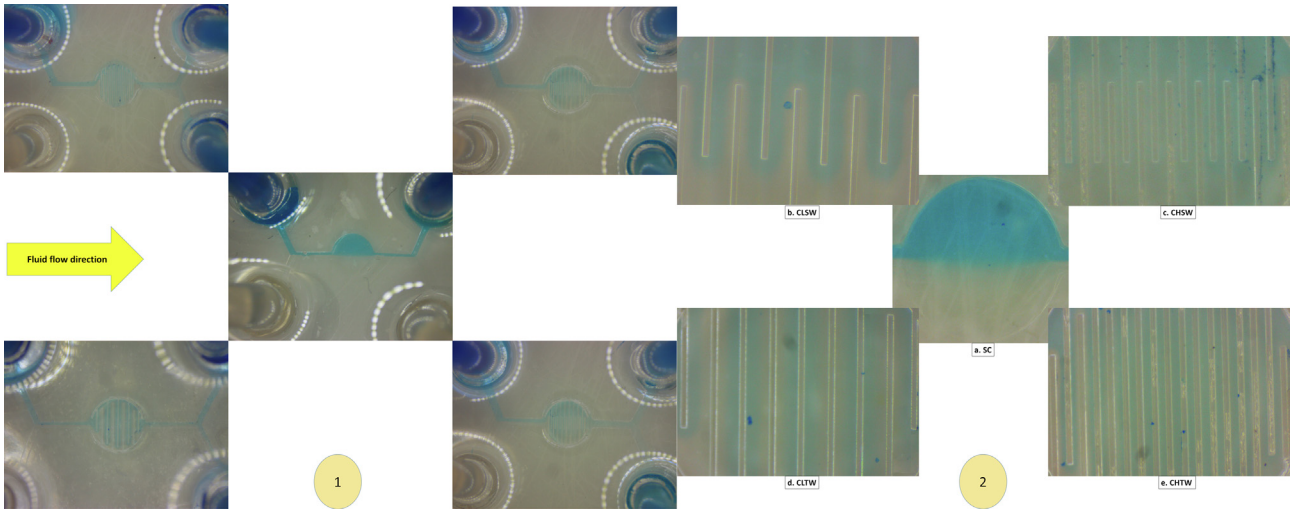

Fig. 5. 1: Optical microscope image of whole chips (2 inlets + 2 outlets + mixing unit area) a) simple circle [SC], b) circle with low number and same level walls [CLSW], c) circle with high number and same level walls [CHSW], d) circle with low number and e) tall walls [CLTW] and circle with high number and tall walls [CHTW] respectively. 2: Zoom in for the mixing unit area, a. SC, b. CLSW, c. CHSW, d. CLTW and e. CHTW, respectively.

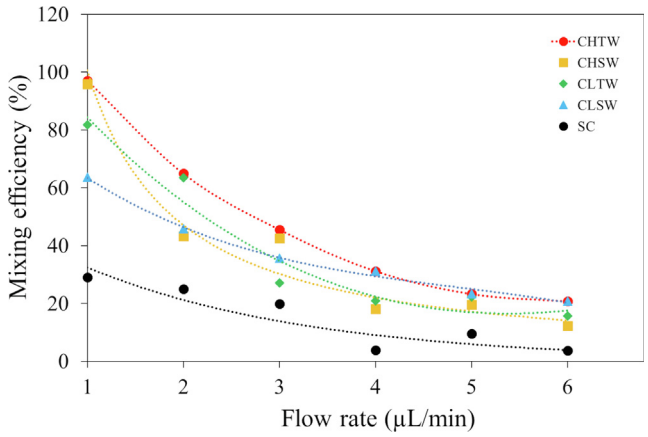

Fig. 6. Mixing efficiency VS flow rate of different wall micromixers: a) simple circle [SC], b) circle with low number and same level walls [CLSW], c) circle with high number and same level walls [CHSW], d) circle with low number and e) tall walls [CLTW] and circle with high number and tall walls [CHTW].

designed in the simulations to improve the mixing efficiency of the chips.

From our earlier work, it was found that the so called micro-wall-array is a promising candidate for passive mixing tasks. In the present work, the length and the areal density of these walls were varied in order to find a better mixing performance. The results showed that, generally, the more densely distributed and the longer walls are more efficient and their combination (long walls, densely distributed) showed the highest performance.

The devices were then created with ion microlithography and UV lithography techniques. Mixing test were performed from which the mixing efficiencies were determined. It was found, that the mixing efficiency of the fabricated passive micromixers, the densely distributed short walls and the densely distributed long walls, improves to an excellent value of 95.86 % and 97.08 %, 1 μl/min flow rate. From these results, we conclude that the distribution of the walls has the higher effect on the mixing.

The basic principle of our chips are that the fluid flow forced to a very narrow "serpentine" shape, where the width of these serpentine are small enough to make the cross diffusion path very low, so the mixing by diffusion will be high and quick. We could make this with micro structures created with proton beam lithography, with which smaller structures can be created than just with UV lithography method. Furthermore, with this construction method we can keep the mixing chip at the same size, and can control the parameters of the serpentine. Therefore, if we work with a smaller molecule we can make a less densely distributed wall chip, getting less pressure drop, or in case of higher molecules we can make more densely distributed chips, in the same basic sizes.

In conclusion, the parameters of the serpentines can easily be controlled, keeping the same chip size.

CRediT authorship contribution statement

Emad Nady: Methodology, Writing – original draft, Investigation, Formal analysis, Validation. **Gyula Nagy:** Writing – original draft, Formal analysis, Validation. **Róbert Huszánk:** Conceptualization, Methodology, Resources, Writing – review & editing, Supervision, Project administration, Funding acquisition, Validation.

Declaration of Competing Interest

The authors declare that they have no known competing financial interests or personal relationships that could have appeared to influence the work reported in this paper.

Acknowledgement

This work was supported by the European Regional Development Fund and Hungary in the frame of the project GINOP-2.2.1-15-2016-00012. Róbert Huszánk is grateful for the János Bolyai Scholarship of the Hungarian Academy of Sciences and the ÚNKP-19-4 New National Excellence Program of the Ministry for Innovation and Technology.

References

Beebe, D.J., Mensing, G.A., Walker, G.M., 2002. Physics and application of microfluidic in biology. Annu. Rev. Biomed. Eng. 4, 261–286.
Hessel, V., Hardt, S., Löwe, H., Schönfeld, F., 2003. Laminar mixing in different interdigital micromixers: I. Experimental characterization. AIChE J. 49 (3), 566–577.

Sullivan, S.P., Akpa, B.S., Matthews, S.M., Fisher, A.C., Gladden, L.F., Johns, M.L., 2007. Simulation of miscible diffusive mixing in microchannels. Sens. Actuators, B 123 (2), 1142–1152.
Knight, J.B., Vishwanath, A., Brody, J.P., Austin, R.H., 1998. Hydrodynamic focusing on a silicon chip: mixing nanoliters in microseconds. Phys. Rev. Lett. 80 (17), 3863–3866.
Bessoth, F.G., deMello, A.J., Manz, A., 1999. Microstructure for efficient continuous flow mixing. Anal. Commun. 36 (6), 213–215.
A.D. Stroock, S.K.W. Dertinger, A. Ajdari, I. Mezí c, H.A. Stone, G.M. Whitesides. (2002). Chaotic mixer for microchannels, Science 295, 647–651.
Wang, Lilin, Yang, Jing-Tang, Lyu, Ping-Chiang, 2007. An overlapping crisscross micromixer. Chem. Eng. Sci. 62 (3), 711–720.
Hassell, D.G., Zimmerman, W.B., 2006. Investigation of the convective motion through a staggered herringbone micromixer at low Reynolds number flow. Chem. Eng. Sci. 61 (9), 2977–2985.
Fu, Xin, Liu, Sufen, Ruan, Xiaodong, Yang, Huayong, 2006. Research on staggered oriented ridges static micromixers. Sens. Actuators, B 114 (2), 618–624.
Sato, Hironobu, Ito, Seiki, Tajima, Kenji, Orimoto, Norimune, Shoji, Shuichi, 2005. PDMS microchannels with slanted grooves embedded in three walls to realize efficient spiral flow. Sens. Actuators, A 119 (2), 365–371.
Yang, Zhen, Matsumoto, Sohei, Goto, Hiroshi, Matsumoto, Mikio, Maeda, Ryutaro, 2001. Ultrasonic micromixer for microfluidic systems. Sens. Actuators, A 93 (3), 266–272.
Bau, Haim H., Zhong, Jihua, Yi, Mingqiang, 2001. Aminute magneto hydro dynamic (MHD) mixer. Sens. Actuators, B 79 (2-3), 207–215.
Lin, Jr-Lung, Lee, Kuo-Hoong, Lee, Gwo-Bin, 2005. Active mixing inside microchannels utilizing dynamic variation of gradient zeta potentials. Electrophoresis 26 (24), 4605–4615.
C. Tsouris, C.T. Culbertson, D.W. DePaoli, S.C. Jacobson, V.F. de Almeida, J.M.Ramsey. (2003). Electrohydrodynamic mixing in microchannels. AIChE J. 49, 2181–2186.
Fu, Lung-Ming, Yang, Ruey-Jen, Lin, Che-Hsin, Chien, Yu-Sheng, 2005. A novel microfluidic mixer utilizing electrokinetic driving forces under low switching frequency. Electrophoresis 26 (9), 1814–1824.
Hong, Chien-Chong, Choi, Jin-Woo, Ahn, Chong H., 2004. A novel in-plane passive microfluidic mixer with modified Tesla structures. Lab-on-a-Chip 4 (2), 109. https://doi.org/10.1039/b305892a.
Liu, Ying Zheng, Kim, Byoung Jae, Sung, Hyung Jin, 2004. Two-fluid mixing in a microchannel. Int. J. Heat Fluid Flow 25 (6), 986–995.
Goullet, Arnaud, Glasgow, Ian, Aubry, Nadine, 2006. Effects of microchannel geometry on pulsed flow mixing. Mech. Res. Commun. 33 (5), 739–746.
Park, Sung-Jin, Kim, Jung Kyung, Park, Junha, Chung, Seok, Chung, Chanil, Chang, Jun Keun, 2004. Rapid three-dimensional passive rotation micromixer using the breakup process. J. Micromech. Microeng. 14 (1), 6–14.
F. Jiang, K.S. Drese, S. Hardt, M. Küpper, F. Schönfeld. (2004). Helical flows and chaotic mixing in curved micro channels. AIChE J. 50, 2297–2305.
Wong, S., Ward, M., Wharton, C., 2004. Micro T-mixer as a rapid mixing micromixer. Sens. Actuators, B 100 (3), 359–379.
Chen, Hao, Meiners, Jens-Christian, 2004. Topologic mixing on amicrofluidic chip. Appl. Phys. Lett. 84 (12), 2193–2195.
Kamholz, A.E. et al., 1999. Quantitative analysis of molecular interactive in microfluidic channel: the T-sensor Anal. Chem. 71, 5340–5347.
Swickrath, Michael J., Burns, Steven D., Wnek, Gary E., 2009. Modulating passive micromixing in 2-D microfluidic devices via discontinuities in surface energy. Sensors Actuators. 140 (2), 656–662.
Bothe, D., Lojewski, A., Warnecke, H.J., 2011. Fully resolved numerical simulation of reactive mixing in a T-shaped micromixer using parabolized species equations. Chem. Eng. Sci. 66, 6424–6440.
Hossain, S., Ansari, M.A., Kim, K.Y., 2009. Evaluation of the mixing performance of three passive micromixers. Chem. Eng. J. 150, 492–501.
Tofteberg, Terje, Skolimowski, Maciej, Andreassen, Erik, Geschke, Oliver, 2010. A novel passive micromixer: lamination in a planar channel system. Microfluid. Nanofluid. 8 (2), 209–215.
Kim, K.Y., Ansari, M.A., 2007. Shape optimization of a micromixer with staggered herringbone groove. Chem. Eng. Sci. 62, 6687–6695.
Kim, K.Y., Hossain, S., Husain, A., 2010. Shape optimization of a micromixer with staggered-herringbone grooves patterned on opposite walls. Chem. Eng. J. 162, 730–737.
Shih T. R. and Chung C. K. (2008). A high-efficiency planar micromixer with convection and diffusion mixing over a wide Reynolds number range Microfluid. Nanofluid. J. 5 175–83.
Xu, Zhongbin, Li, Chunhui, Vadillo, Damien, Ruan, Xiaodong, Fu, Xin, 2011. Numerical simulation on fluid mixing by effects of geometry in staggered oriented ridges micromixers. Sensors Actuators B. 153 (1), 284–292.
Cho, H.H., Kim, B.S., Kwak, B.S., Shin, S., Lee, S., Kim, K.M., Jung, H.I., 2011. Optimization of microscale vortex generators in a microchannel using advanced response surface method. Int. J. Heat Mass Transf. 54, 118–125.
Yu, X., Lin, Y., Wang, Z., Tu, S.T., Wang, Z., 2011. Design and evaluation of an easily fabricated micromixer with three-dimensional periodic perturbation. Chem. Eng. J. 171, 291–300.
Ohkawa, K. et al., 2008. Flow and mixing characteristics of σ –type plate static mixer with splitting and inverse recombination. Chem. Eng. Res. Des. 86, 1447–1453.
Lee, Seok Woo, Lee, Seung S., 2008. Rotation effect in split and recombination micromixing. Sensors Actuators B 129 (1), 364–371.
Chen Z., Bown M. R., Sullivan B. O., MacInnes J. M., Allen R. W. K., Mulder M., Blom M. and van't Oever R. (2009). Performance analysis of a folding flow micromixer. Microfluid. Nanofluid. 6 763–74.
Chen, J.J., Lai, Y.R., Tsai, R.T., Lin, J.D., Wu, C.Y., 2011. Crosswise ridge micromixers with split and recombination helical flows. Chem. Eng. Sci. 66, 2164–2176.
Nimafar, M., Viktorov, V., Martinelli, M., 2012. Experimental comparative mixing performance of passive micromixers with H-shaped sub-channels. Chem. Eng. Sci. 76, 37–44.
Cai, Gaozhe, Xue, Li, Zhang, Huilin, Lin, Jianhan, 2017. A Review on Micromixers. Micromachines 8, 274–301.
Karthikeyan, K., Sujatha, L., Sudharsan, N.M., 2017. Numerical Modeling and Parametric Optimization of Micromixer for Low Diffusivity Fluids. Int. J. Chem. Reactor Eng. 16 (3), 20160231.
Nimafar, Mohammad, Viktorov, Vladimir, Martinelli, Matteo, 2012. Experimental Investigation of Split and Recombination Micromixer in Confront with Basic T- and O- Type Micromixers. Int. J. Mechanics Applications 2 (5), 61–69.
Alam, Afroz, Afzal, Arshad, Kim, Kwang-Yong, 2014. Mixing Performance of a Planar Micromixer with Circular Obstructions in a Curved Microchannel. Chem. Eng. Res. Des. 92 (3), 423–434.
Afzal, Arshad, Kim, Kwang-Yong, 2014. Three-Objective Optimization of a Staggered Herringbone Micromixer. Sens. Actuators, B 192, 350–360.
Jen, Chun-Ping, Wu, Chung-Yi, Lin, Yu-Cheng, Wu, Ching-Yi, 2003. Design and Simulation of the Micromixer with Chaotic Advection in Twisted Microchannels. Lab Chip 3 (2), 77. https://doi.org/10.1039/b211091a.
Tung, Kai-Yang, Li, Chih-Chieh, Yang, Jing-Tang, 2009. Mixing and Hydrodynamic Analysis of a Droplet in a Planar Serpentine Micromixer. Microfluid. Nanofluid. 7 (4), 545–557.
Madhumitha, R., Arunkumar, S., Karthikeyan, K.K., Krishnah, S., Ravichandran, V., Venkatesan, M., 2017. Computational Modeling and Analysis of Fluid Structure Interaction in Micromixers with Deformable Baffle. Int. J. Chem. Reactor Eng. 15 (3), 20160121.
Chen, Xueye, Wang, Xiaolei, 2015. Optimized Modular Design and Experiment for Staggered Herringbone Chaotic Micromixer. Int. J. Chem. Reactor Eng. 13 (3), 305–309.
Wang, Chin-Tsan, Chen, Yan-Ming, Chen, Shih-Syun, 2016. Heart-Like Micro-Flow Mixer. Int. J. Chem. Reactor Eng. 14 (1), 343–349.
Wang, Chin-Tsan, Chen, Yan-Ming, Hong, Pei-An, Wang, Yi-Ta, 2014. Tesla Valves in Micromixers. Int. J. Chem. Reactor Eng. 12 (1), 397–403.
Cha, Junghun, Kim, Jinseok, Ryu, Suk-Kyu, Park, Jungyul, Jeong, Yongwon, Park, Sewan, Park, Sukho, Kim, Hyeon Cheol, Chun, Kukjin, 2006. A Highly Efficient 3D Micromixer Using Soft PDMS Bonding. J. Micromech. Microeng. 16 (9), 1778–1782.
Kapilmanoharan, Prabhatranjan, Lekurwale, Ramesh R., 2014. Design & Development of a Micro-Mixer-Reactor for a LOC Application. International Journal of Advances in Science Engineering and Technology 2, 4.
Svasek, P., Svasek, E., Lendl, B., Vellekoop, M., 2004. Fabrication of Miniaturized Fluidic Devices Using SU-8 Based Lithography and Low Temperature Wafer Bonding. Sens. Actuators, A 115 (2-3), 591–599.
Saragih, Agung Shamsuddin, Ko, Tae Jo, 2009. Fabrication of Passive Glass Micromixer with Third-Dimensional Feature by Employing SU8 Mask on Micro-Abrasive Jet Machining. The International Journal of Advanced Manufacturing Technology 42 (5-6), 474–481.
Nady, Emad, Nagy, Gyula, Huszánk, Róbert, 2021. Functionalization of microfluidic devices by microstructures created with proton beam lithography. Vacuum 190, (2021) 110295.